

# Analyst

Accepted Manuscript



This is an *Accepted Manuscript*, which has been through the Royal Society of Chemistry peer review process and has been accepted for publication.

*Accepted Manuscripts* are published online shortly after acceptance, before technical editing, formatting and proof reading. Using this free service, authors can make their results available to the community, in citable form, before we publish the edited article. We will replace this *Accepted Manuscript* with the edited and formatted *Advance Article* as soon as it is available.

You can find more information about *Accepted Manuscripts* in the [Information for Authors](#).

Please note that technical editing may introduce minor changes to the text and/or graphics, which may alter content. The journal's standard [Terms & Conditions](#) and the [Ethical guidelines](#) still apply. In no event shall the Royal Society of Chemistry be held responsible for any errors or omissions in this *Accepted Manuscript* or any consequences arising from the use of any information it contains.

# Pre-Equilibration Kinetic Size-Exclusion Chromatography with Mass Spectrometry Detection (peKSEC-MS) for Label-Free Solution-Based Kinetic Analysis of Protein-Small Molecule Interactions

Jiayin Bao,<sup>a</sup> Svetlana M. Krylova,<sup>a</sup> Leonid T. Cherney,<sup>a</sup> J.C. Yves Le Blanc,<sup>b</sup> Patrick Pribil,<sup>b</sup> Philip E. Johnson,<sup>a</sup> Derek J. Wilson<sup>a</sup> and Sergey N. Krylov<sup>a\*</sup>

**Here we introduce pre-equilibration kinetic size-exclusion chromatography with mass-spectrometry detection (peKSEC-MS), which is a label-free solution-based kinetic approach for characterizing non-covalent protein-small molecule interactions. In this method, protein and small molecule are mixed outside the column and incubated to approach equilibrium. The equilibrium mixture is then introduced to the SEC column to initiate the dissociation process by separating small molecule from the complex inside the column. A numerical model of 1-dimensional separation was built to simulate the mass-chromatograms of small molecule for varying rate constants of binding.**

Non-covalent protein small molecule interactions are critical in regulating various biological processes.<sup>1-3</sup> Additionally, in drug development, the small molecules are often designed to change protein functions through non-covalent binding.<sup>4-6</sup> Knowing the kinetic rate constants of protein-small molecule interaction is essential in understanding cellular processes and the functions of drugs.<sup>7-10</sup> In a schematic sense, we need to know rate constants  $k_{on}$  and  $k_{off}$  of the following reaction involving a protein (P), a small molecule (SM), and a protein-small molecule complex (P-SM):



The equilibrium dissociation constant can be calculated through  $K_d = k_{off}/k_{on}$  (smaller  $K_d$  value indicates high affinity binding).

The majority of practical methods for measuring kinetic rate constants of protein-small molecule interaction require modification of either P or SM. In general these methods can be categorized into 2 groups: label-based and surface-based. Label-based methods, for example stopped-flow spectroscopy,<sup>11,12</sup> require attachment of a spectroscopically active molecule, such as a fluorophore, onto either P or SM. The surface-based methods, such as surface plasmon resonance (SPR)<sup>13,14</sup> and bio-layer interferometry,<sup>15,16</sup> require immobilization of either P or SM onto an optical sensor. Moreover, the most sensitive mode of detection requires the immobilization or labeling of the small molecule rather than the protein.<sup>17,18</sup> Modifications of small molecules are difficult to achieve, and they can also drastically affect protein-small molecule binding. Therefore, the label-free solution-based kinetic methods are needed for simple and accurate measurements of  $k_{on}$  and  $k_{off}$ .

Recently we have introduced a solution-based, label-free approach for kinetic analysis of non-covalent protein-small molecule interaction called kinetic size-exclusion chromatography

(KSEC-MS).<sup>19</sup> In KSEC-MS, generic solution-based kinetic separation is realized in a size-exclusion chromatography (SEC) column; label-free detection of SM is done with tandem mass spectrometry (MS/MS). The shape of the resulting chromatogram, signal (proportional to SM concentration) *versus* time, is defined by  $k_{on}$  and  $k_{off}$ . The values of  $k_{on}$  and  $k_{off}$  can be determined by finding a suitable mathematical model and fitting the experimental chromatogram with simulated ones while varying  $k_{on}$  and  $k_{off}$ . The best fit reveals the appropriate values of  $k_{on}$  and  $k_{off}$ . Plug-plug kinetic size-exclusion chromatography mass spectrometry (ppKSEC-MS) was our first practical implementation of the KSEC-MS concept. In essence, short plugs of SM and P are separately injected into the column; SM is followed by P. In a SEC column, P moves faster, and during the plug of P's passing through the plug of SM, the binding reaction occurs and the P-SM complex is formed. When P outruns SM, the continuous dissociation of the complex starts. We developed a 1-dimensional numerical model for simulating a ppKSEC-MS chromatogram, and used it to find  $k_{on}$  and  $k_{off}$  for the interaction of carbonic anhydrase and its inhibitor, acetazolamide.

To further develop the idea of label-free solution-based kinetic measurements, we now introduce the next KSEC-MS method, pre-equilibration kinetic size-exclusion chromatography (peKSEC). The concept of peKSEC is depicted in Fig. 1. An "equilibrium mixture" (EM) is made by incubating P with SM to approach equilibrium shown in Reaction 1. A small volume of the EM (much smaller than free volume of the column) is injected into a SEC column at time  $t_0$  and its components are separated based on their size differences. As soon as SM is separated from P-SM, the latter is no longer at equilibrium and starts dissociating releasing more unbound SM. The dissociation process continues leaving a "tail" of SM. The samples in column will eventually elute in the following order: (i) the intact P-SM, (ii) the "tail" of SM that dissociated from complex during separation, and (iii) the unbound SM in the EM. Upon leaving the column the small molecule can be ionized by various ionization methods, such as electrospray ionization (ESI) or atmospheric-pressure chemical ionization (APCI), and detected.<sup>20</sup> During ionization, the intact P-SM is deliberately destroyed, thus SM from the complex is freed and also detected by MS/MS. In general, a peKSEC-MS chromatogram contains 3 features: (i) a peak that corresponds to SM that exited the column as a part of the intact P-SM, (ii) a peak of SM that was unbound in EM, and (iii) a bridge between the two peaks that corresponds to SM that was bound to P but dissociated during separation. The shapes and areas of these three features are defined by  $k_{on}$  and  $k_{off}$ . Accordingly, fitting the chromatogram with a 1-dimensional mathematical model that describes reaction 1 along with mass transfer in the chromatographic column reveals both rate constants  $k_{on}$  and  $k_{off}$ .

<sup>a</sup>Department of Chemistry and Centre for Research on Biomolecular Interactions, York University, Toronto, Ontario M3J 1P3, Canada

<sup>b</sup>AB Sciex, 71 Four Valley Dr, Vaughan, Ontario L4K 4V8, Canada  
E-mail: skrylov@yorku.ca; Tel: +416-736-2100 ext 22345

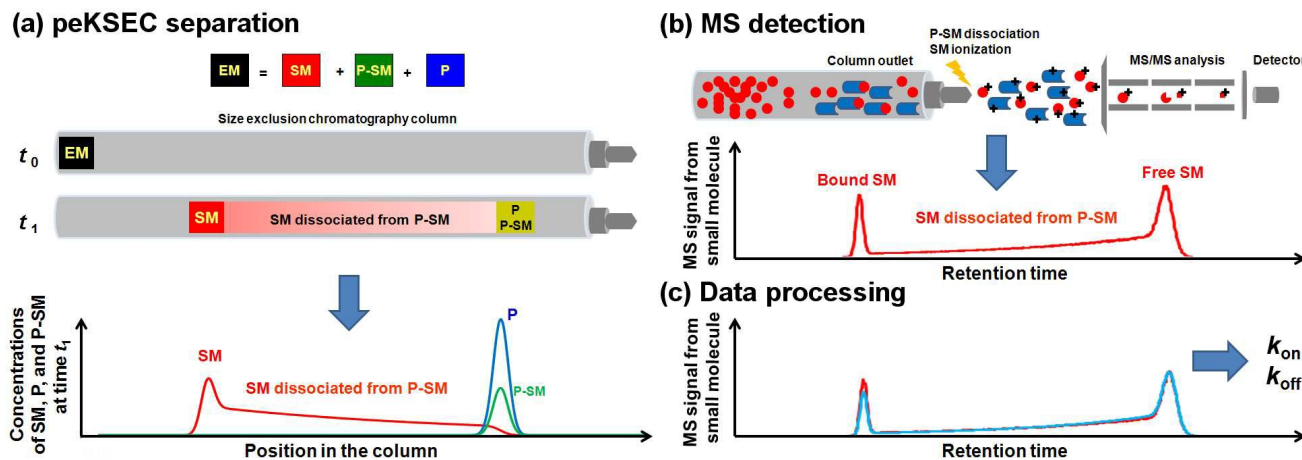


**Fig. 1** Conceptual depiction of separation (a), detection (b), and data processing (c) in peKSEC. (a): The EM contains P, SM, and P-SM at equilibrium concentrations. EM is sampled into a SEC column at time  $t_0$ . P and P-SM are large and, therefore, move faster than SM and practically together as the size difference between them is negligible. When SM leaves the zone of P-SM, the equilibrium is disrupted and complex starts dissociating. The newly released SM is continuously separated from P-SM and forms a bridge between the zones of P/P-SM and SM shown at time  $t_1$ . The graph illustrates the corresponding concentrations of P, SM, and P-SM at time  $t_1$ . (b): The eluate from SEC column is continuously sampled into a mass spectrometer tuned to detect SM. The P-SM dissociates during ionization to release SM which facilitates indirect detection of the intact P-SM. The resulting KSEC chromatogram contains two peaks and a bridge between them. The fastest peak corresponds to intact P-SM reaching the end of the column and the slowest one corresponds to SM that was unbound in EM. The bridge corresponds to SM that dissociated from P-SM during the separation. (c): The experimental chromatogram is numerically fitted with a system of partial differential equations describing the processes of chromatographic separation and reaction 1. The values of  $k_{on}$  and  $k_{off}$  are used as fitting parameters and the best fit corresponds to the sought correct values of  $k_{on}$  and  $k_{off}$ .

The great strength of peKSEC-MS is that it relies on a generic separation as a small molecule can always be separated from a large P-SM complex. Moreover, peKSEC-MS uses a generic detection scheme, as practically any small molecule can be selectively detected by MS/MS. Here, we chose the interaction between dihydrofolate reductase (DHFR) with methotrexate (MTX) as a model system. DHFR is an essential enzyme in cell proliferation and cell growth; it converts dihydrofolic acid to tetrahydrofolic acid, and MTX is its well known inhibitor.<sup>21-23</sup> DHFR and MTX can be easily separated by SEC based on the difference in their sizes. The MS/MS signal intensity of MTX was proportional to the concentration in a range of 10  $\mu\text{M}$  – 100 pM; the linear response in the nanomolar range is essential for studying high affinity binding (nanomolar  $K_d$ ). When EM of DHFR and MTX was sampled with detection for MTX only, a predicted peKSEC-MS chromatogram was obtained in Fig. 2. The signal intensity of the leftmost peak, which corresponds to P-SM increased with increasing protein concentration [P] in EM. A similar trend was also observed for the bridge region, which corresponds to SM that dissociated from P-SM during separation. Meanwhile, as we anticipated, the rightmost peak, free SM, decreased with increasing [P] in EM. The integral of the SM signal over the entire chromatogram remained constant with changing [P] (and the concentration of small molecule [SM] remained constant) suggesting that the intact complex was completely dissociated and all SM was accounted for.

Deconvolution of the kinetic rate constants from a peKSEC-MS chromatogram is not a trivial task. While no analytical solutions are available, we have adapted the numerical approach previously developed for modeling ppKSEC-MS to model processes in peKSEC-MS. It is a 1-dimensional model that considers complex dissociation and complex re-formation during migration of the components through the column. The following setup is used for the 1-dimensional approach in peKSEC-MS. A long and narrow cylindrical chromatography column is coaxial with the x coordinate. It is filled with the beads that constitute the stationary phase. The beads have pores which are, in the first

approximation, large enough for the SM to enter and reside inside for significant time and too small for the P or the P-SM to be significantly retarded. This is confirmed by the significant difference in retention times between SM and P-SM. Also, the model uses an assumption of fast re-equilibration between the mobile and stationary phase, which is confirmed by narrow peaks of P and SM. An EM plug containing SM, P, and P-SM is injected into the column at  $t = 0$  ( $t_0$ ). We assume that the buffer velocity and concentrations of components P and P-SM are averaged across the column over the area lying outside the beads. Similarly, the concentrations of SM outside the beads and inside them are averaged across the column over the area lying outside the beads and inside the pores, respectively. Mass transfers of SM, P, and P-SM are described by the following equations

$$(\partial_t + v_{SM}\partial_x - D_{SM}\partial_x^2)[SM] = \alpha(k_{off}[P-SM] - k_{on}[SM][P]) \quad (2)$$

$$(\partial_t + v\partial_x - D_p\partial_x^2)[P] = k_{off}[P-SM] - k_{on}[SM][P] \quad (3)$$

$$(\partial_t + v\partial_x - D_p\partial_x^2)[P-SM] = k_{on}[SM][P] - k_{off}[P-SM] \quad (4)$$

$$v_{SM} = \alpha v, \quad \alpha = \frac{\phi_{out}}{\phi_{out} + \phi_{in}}, \quad D_{SM} = \frac{\phi_{out}D_{out} + \phi_{in}D_{in}}{\phi_{out} + \phi_{in}} \quad (5)$$

Here, [SM], [P], and [P-SM] are the concentrations of the small molecule, protein, and complex, respectively;  $v$  is the average velocity of the buffer;  $D_{out}$  and  $D_{in}$  are diffusion coefficients of SM outside the beads and inside their pores;  $D_p$  is the diffusion coefficient of P and P-SM (we consider them similar since SM does not significantly affect the size of P upon binding);  $\phi_{out}$  and  $\phi_{in}$  are relative volumes (i.e. fractions of the column volume) located outside beads and inside pores, respectively. Average concentrations of SM outside beads and inside pores are considered to be approximately the same due to fast diffusion equilibration between pores and outside the beads volume. Indeed, we usually have  $t_{in} \sim R_{in}^2/D_{in}$  where  $t_{in}$  is the characteristic time of diffusional relaxation between concentrations of small molecules outside the beads and inside their pores and  $R_{in}$  is the characteristic size of the beads. Relation  $t_{in} \sim R_{in}^2/D_{in}$  follows from the fact that Einstein's characteristic diffusion length  $(D_{in}t)^{1/2}$

should be of the order of the characteristic size of beads,  $R_{in}$ , if we calculate this length for the characteristic time of diffusional relaxation  $t \sim t_{in}$ . At  $R_{in} \sim 3 \mu\text{m}$  and  $D_{in} \sim 10^{-5} \text{ cm}^2/\text{s}$  calculations give  $t_{in} \sim 0.01 \text{ s}$ . Thus  $t_{in} \ll t_{sep} = W/(v - v_A)$  where  $t_{sep}$  is the separation time which is usually in the order of a few seconds,  $W$  is the plug length. It should be noted that coefficient  $\alpha$  depends only on the ratio  $\phi_{out}/\phi_{in}$  that coincides with the ratio of actual (not relative) volumes located outside beads and inside pores. We also omitted an additional term proportional to  $t_{in}$ <sup>19</sup> in the last expression (5) for  $D_{SM}$  since we used the fitting procedure to determine  $D_{SM}$ .

To formulate initial conditions for equations 2 – 5 we take into account that the injection usually satisfies the following conditions: (i) the mixture of SM, P, and P-SM is in equilibrium before the injection; (ii)  $t_{inj} \ll t_{eq}$ , where  $t_{inj}$  is the injection time and  $t_{eq} = 1/(k_{on}[P]_0 + k_{off})$  is the equilibration time; and (iii)  $t_{in} \ll t_{inj}$ . In this case, the concentrations in the injected plug at  $t = 0$  (i.e. immediately after injection) are determined by relations:

$$[SM]_0 = \alpha[SM]_{eq}, [P]_0 = [P]_{eq}, [P-SM]_0 = [P-SM]_{eq} \quad (6)$$

$$(0 \leq x \leq W, t = 0)$$

$$W = \frac{V_{inj}}{\pi \phi_{out} R^2}, \quad \phi_{out} = \frac{V_{free}}{\pi R^2 L} \quad (7)$$

Here,  $[SM]_{eq}$ ,  $[P]_{eq}$ , and  $[P-SM]_{eq}$  are concentrations of SM, P, and P-SM in their equilibrium mixture before injection;  $W$  is the plug length after injection;  $V_{inj}$  is the volume of injected mixture;  $V_{free}$  is the free column volume measured by elution of the protein (in the absence of small molecules);  $R$  is the inner radius of the column;  $L$  is the column length. Relations 2 – 7 were used to obtain a numerical solution of the problem and to simulate signal  $S(t)$  generated by SM. We assume that intact P-SM that reaches the end of the column dissociates in mass-spectrometer and SM produced from this dissociation can be detected. As a result  $S(t)$  is proportional to the total concentration of SM (both unbound and bound to P) at the column exit, where  $g$  is a proportionality coefficient:

$$S(t) = g([SM](t) + [P-SM](t)) \quad (8)$$

The model was implemented in COMSOL multi-physics software (4.3a commercial software). The kinetic rate constants  $k_{on}$  and  $k_{off}$  were convoluted to form simulated chromatogram. Non-linear regression was used to find the best fit of the experimental peKSEC-MS chromatogram by the simulated one. By fitting the experimental chromatograph to 1-dimensional model we have calculated the kinetic rate constants:  $k_{on} = (57.2 \pm 3.5) \times 10^4 \text{ M}^{-1}\text{s}^{-1}$ ,  $k_{off} = (47.2 \pm 4.6) \times 10^{-4} \text{ s}^{-1}$ , and  $K_d = (8.2 \pm 1.3) \times 10^{-9} \text{ M}$  was calculated through  $k_{off}/k_{on}$ . The best fits for different chromatograms (Fig. 2) returned similar values of  $k_{on}$  and  $k_{off}$  suggesting that the solution is stable and also allowing us to estimate method's precision. To validate our results, we chose another label free solution based method ITC (Fig. 3). ITC is an equilibrium method from which only  $K_d$  can be calculated;<sup>24</sup> it was selected due to the lack of other label-free kinetic method. ITC and peKSEC-MS are conceptually different methods, offering a means of validation with higher stringency. The ITC measured equilibrium dissociation constant  $K_d = (10.2 \pm 0.8) \times 10^{-9} \text{ M}$ , which agreed with peKSEC-MS measured results within error, thus confirmed the accuracy of peKSEC-MS.

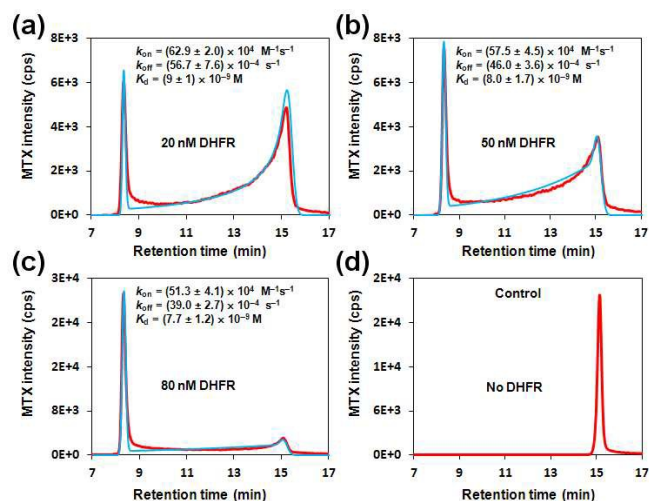


**Fig. 2** The peKSEC analysis of DHFR-MTX binding interactions. There are 20 nM MTX mixed with different concentrations of DHFR (a) to (c). The control (d) contains MTX only. The MTX signal was detected with MS/MS for 455.2/308.2 (Q1/Q3) m/z. Simulation chromatograms (blue) were generated from modeling the processes involved in peKSEC by using COMSOL multi-physics software. The kinetic rate constants were determined from the best fit of the experimental chromatogram (red) by the simulated one, and were calculated based on the average and standard deviation of triplicated results.

## Conclusions

To conclude, we have outlined the main features of peKSEC-MS, which is a label-free solution-based method for studying kinetics of reversible binding between a protein and a small molecule. In peKSEC, the migration pattern of the small molecule through a SEC column is followed with MS detection, and the kinetic parameters are extracted from the MS signal versus time dependence by means of numerical modelling. The numerical model uses two assumptions: (i) complex dissociation is complete during the ionization and (ii) the ionization efficiency of small molecule remains constant. In essence, we assume that the linear response of MS to small molecule concentration is retained throughout the analysis. The requirement of complete dissociation is easily satisfied as it is difficult to keep non-covalent complexes intact during the ionization process. The second assumption may not be always satisfied; for example, the ionization efficiency of small molecule could be affected when it co-elutes with the protein.<sup>25</sup> Therefore, it is essential to confirm the method validity by comparing the integrated small molecule signals among all tests – it should remain constant for constant small molecule concentration and not depend on the concentration of the protein. Moreover, measuring fast reactions with low  $K_d$  values will require low concentrations of interacting molecules and accordingly lower detection limit of MS.<sup>26-28</sup> The sub-nanomolar  $K_d$  measurements will require a mass spectrometer with a sub-nanomolar detection limit. Instrumentation for peKSEC-MS used in this study can measure small molecule concentration of 100 pM and the best contemporary MS instruments have limits of detection in the zeptomolar range.<sup>29</sup> Advantageously, peKSEC-MS does not require MS detection of an intact protein-small molecule complex, which may be very challenging. The ability of MS to rapidly scan through a wide mass range can potentially facilitate simultaneous analysis of one protein with several small molecules that potentially can be used for the rapid screening of panels of drug leads. The peKSEC method allows tight control of



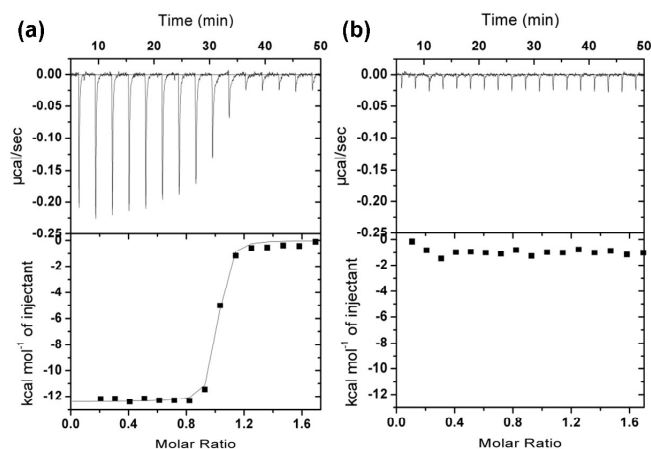


**Fig. 3** Thermograms of binding analysis between DHFR and MTX by ITC. (a): titrating DHFR with MTX and (b): titrating DHFR with buffer only. The upper graphs show the raw ITC data in real time and the lower graphs show the corresponding integrated total heat per injection with respect to molar ratio. The fitting was generated by using Origin 5.0 software with a single-binding-site model.

binding conditions such as incubation time and temperature, presence of cofactors, etc. Furthermore, as peKSEC relies on the established equilibrium prior to injection, we can now analyze the protein-small molecule interactions with slow association rates. Whereas in ppKSEC, the on-column incubation of slow interacting pair is impractical, and can also induce sample diffusion and peak broadening. We foresee that peKSEC-MS can become a generic solution-based label-free platform for kinetic studies of protein-small molecule interactions.

## Supporting Information

This material is available free of charge via the Internet.

## Acknowledgments

The authors thank Prof. Dasantila Golemi-Kotra for facilitating ITC measurements.

This work was funded by the Natural Sciences and Engineering Research Council of Canada.

## Notes and references (titles are left for convenience of reviewers)

1. B. Z. Stanton, L. F. Peng, *Mol. BioSyst.* 2010, **6**, 44-54. (Small-molecule modulators of the Sonic Hedgehog signaling pathway)
2. K. Vrijens, W. Lin, J. Cui, D. Farmer, J. Low, E. Pronier, F. Zeng, A. A. Shelat, K. Guy, M. R. Taylor, T. Chen, M. F. Roussel, *PLoS ONE* 2013, **8**, e59045. (Identification of small molecule activators of bmp signaling)
3. A. J. Firestone, J. K. Chen, *ACS Chemical Biol.* 2010, **5**, 15-34. (Controlling destiny through chemistry: small-molecule regulators of cell fate)
4. J. Zhang, P. L. Yang, N. S. Gray, *Nat. Rev. Cancer* 2009, **9**, 28-39. (Targeting cancer with small molecule kinase inhibitors)
5. S. Shangary, S. Wang, *Annu. Rev. Pharmacol. Toxicol.* 2009, **49**, 223-241. (Small-molecule inhibitors of the MDM2-p53 protein-protein interaction to reactivate p53 function: a novel approach for cancer therapy)

6. D. V. Dabir, S. A. Hasson, K. Setoguchi, M. E. Johnson, P. Wongkongkathep, C. J. Douglas, J. Zimmerman, R. Damoiseaux, M. A. Teitell, C. M. Koehler, *Developmental Cell* 2013, **25**, 81-92. (A small molecule inhibitor of redox-regulated protein translocation into mitochondria)
7. R. A. Copeland, *Expert Opin. Drug Discov.* 2010, **5**, 305-310. (The dynamics of drug-target interactions: drug-target residence time and its impact on efficacy and safety)
8. H. Lu, P. J. Tonge, *Curr. Opin. Chem. Biol.* 2010, **14**, 467-474. (Drug-target residence time: critical information for lead optimization)
9. D. C. Swinney, *Drug Disc.* 2010, **7**, 53-57. (Influence of drug binding kinetics on pharmacodynamic properties)
10. P. Imming, C. Sinning, A. Meyer, *Nat. Rev. Drug Discov.* 2006, **5**, 821-834. (Drugs, their targets and the nature and number of drug targets)
11. R. Murugan, S. Mazumdar, *Arch. Biochem. Biophys.* 2006, **15**, 154-162. (Effect of alcohols on binding of camphor to cytochrome P450cam: spectroscopic and stopped flow transient kinetic studies)
12. P. T. R. Rajagopalan, Z. Zhang, L. McCourt, M. Dwyer, S. Benkovic, G. G. Hammes, *Proc. Natl. Acad. Sci. U. S. A.* 2002, **99**, 13481-13486. (Integration of dihydrofolate reductase with methotrexate: Ensemble and single-molecule kinetics)
13. A. M. Cooper, *Nat. Rev. Drug Discov.* 2002, **1**, 515-528. (Optical biosensor in drug discovery)
14. D. G. Myszka, *Anal. Biochem.* 2004, **329**, 316-323. (Analysis of small-molecule interactions using Biacore S51 technology)
15. Y. Fang, *Expert Opin. Drug Discov.* 2012, **7**, 969-988. (Ligand-receptor interaction platforms and their applications for drug discovery)
16. C. A. Wartchow, F. Podlaski, S. Li, K. Rowan, X. Zhang, D. Mark, K. Huang, *J. Comput. Aided Mol. Des.* 2011, **25**, 669-676. (Biosensor-based small molecule fragment screening with bilayer interferometry)
17. N. Kanoh, M. Kyo, K. Inamori, A. Ando, A. Asami, A. Nakao, H. Osada, *Anal. Chem.* 2006, **78**, 2226-2230. (SPR Imaging of photo-cross-linked small-molecule arrays on gold)
18. R. P. H. Kooyman, In: *Handbook of Surface Plasmon Resonance*. Eds. R.B.M Schasfoort, A.J. Tudos. RSC Publishing 2008, pp. 15-35. (Physics of surface plasmon resonance)
19. J. Bao, S. M. Krylova, L. T. Cherney, J. C. Y. LeBlanc, P. Pribil, P. E. Johnson, D. J. Wilson, S. N. Krylov, *Anal. Chem.* 2014, **86**, 10016-10020. (Kinetic size-exclusion chromatography with mass spectrometry detection: an approach for solution-based label-free kinetic analysis of protein-small molecule interactions)
20. B. L. Ackermann, M. J. Berna, J. A. Eckstein, L. W. Ott, A. K. Chaudhary, *Annu. Rev. Anal. Chem.* 2008, **1**, 357-396. (Current applications of liquid chromatography/mass spectrometry in pharmaceutical discovery after a decade of innovation)
21. I. Batruch, E. Javasky, E. D. Brown, M. G. Organ, P. E. Johnson, *Bioorgan. Med. Chem.* 2010, **18**, 8485-8492. (Thermodynamic and NMR analysis of inhibitor binding to dihydrofolate reductase)
22. R. L. Summerfield, D. M. Daigle, S. Mayer, D. Mallik, D. W. Hughes, S. G. Jackson, M. Sulek, M. G. Organ, E. D. Brown, M. S. Junop, *J. Med. Chem.* 2006, **49**, 6977-6986. (A 2.13 Å structure of e. coli dihydrofolate reductase bound to a novel competitive inhibitor reveals a new binding surface involving the m20 loop region)
23. M. A. Wani, X. Xu, P. J. Stambrook, *Cancer Res.* 1994, **54**, 2504-2508. (Increased methotrexate resistance and dhfr gene amplification as a consequence of induced ha-ras expression in nih 3t3 cells)
24. C. T. Liu, P. Hanobian, J. B. French, T. H. Pringle, S. Hammes-Schiffer, S. J. Benkovic, *Proc. Natl. Acad. Sci. U. S. A.*, 2013, **110**, 10159-10164. (Functional significance of evolving protein sequence in dihydrofolate reductase from bacteria to humans)
25. B. K. Matuszewski, M. L. Constanzer, C. M. Chaves-Eng, *Anal. Chem.* 2003, **75**, 3019-3030. (Strategies for the assessment of matrix effect in quantitative bioanalytical methods based on hplc-ms/ms)

- 1  
2  
3  
4  
5  
6  
7  
8  
9  
10  
11  
12  
13  
14  
15  
16  
17  
18  
19  
20  
21  
22  
23  
24  
25  
26  
27  
28  
29  
30  
31  
32  
33  
34  
35  
36  
37  
38  
39  
40  
41  
42  
43  
44  
45  
46  
47  
48  
49  
50  
51  
52  
53  
54  
55  
56  
57  
58  
59  
60
26. J. Bao, S. M. Krylova, D. J. Wilson, O. Reinstein, P. E. Johnson, S. N. Krylov, *ChemBioChem* 2011, **12**, 2551–2554. (Kinetic Capillary Electrophoresis with Mass-Spectrometry Detection (KCE-MS) Facilitates Label-Free Solution-Based Kinetic Analysis of Protein–Small Molecule Binding)
  27. J. Bao, S. M. Krylova, O. Reinstein, P. E. Johnson, S. N. Krylov, *Anal. Chem.* 2011, **83**, 8387–8390. (Label-Free Solution-Based Kinetic Study of Aptamer–Small Molecule Interactions by Kinetic Capillary Electrophoresis with UV Detection Revealing How Kinetics Control Equilibrium)
  28. M. Berezovski, S. N. Krylov, *J. Am. Chem. Soc.* 2002, **124**, 13674–13675. (Nonequilibrium capillary electrophoresis of equilibrium mixtures - a single experiment reveals equilibrium and kinetic parameters of protein-DNA interactions)
  29. M. E. Belov, M. V. Gorshkov, H. R. Udseth, G. A. Anderson, R. D. Smith, *Anal. Chem.*, 2000, **72**, 2271–2279. (Zeptomole-Sensitivity Electrospray Ionization–Fourier Transform Ion Cyclotron Resonance Mass Spectrometry of Proteins)

1  
2  
3  
4  
5  
6  
7  
8  
9  
10  
11  
12  
13  
14  
15  
16  
17  
18  
19  
20  
21  
22  
23  
24  
25  
26  
27  
28  
29  
30  
31  
32  
33  
34  
35  
36  
37  
38  
39  
40  
41  
42  
43  
44  
45  
46  
47  
48  
49  
50  
51  
52  
53  
54  
55  
56  
57  
58  
59  
60